JOURNAL OF SOLID STATE CHEMISTRY 39, 314–328 (1981)

# The Structure of Cubic $YbZrF_7$

MARCEL POULAIN

*Laboratoire de Chimie Minérale D, Laboratoire associé au CNRS No. 254, Université de Rennes I, 35042 Rennes, France*

AND BRUCE C. TOFIELD

*Materials Development Division, AERE Harwell, Oxon, OX11 ORA, United Kingdom*

Received March 17, 1981

The structure of primitive-cubic $YbZrF_7$ has been determined using X-ray and neutron diffraction techniques. A unit cell ($a$ = 4.07 Å, space group $Pm3m$) contains one formula unit of $Yb_{0.5}Zr_{0.5}F_{3.5}$, with no ordering of cations, in materials prepared by rapid quenching from 1000°C. Metal and fluorine displacements from ideal sites are in accord with results previously obtained on $Zr_{0.8}Yb_{0.2}F_{3.2}O_{0.3}$. The separation between F–F pairs bridging neighboring metal ions is similar to those observed in other complex zirconium fluorides. The metal displacements, metal–fluorine distances and fluorine–fluorine distances are discussed with respect to the formation and stability of disordered fluorine-excess $ReO_3$-type phases. These materials are intermediate in character between phases such as monoclinic $YbZrF_7$, with perfect order on both metal and nonmetal sublattices, and $ZrF_4$-based glasses where there is disorder on the metal as well as on the fluorine sublattice. No ordering effects are observed on heating to near 200°C, but near 400°C there is a slow transformation to the monoclinic $YbZrF_7$ structure.

## Introduction

We have recently demonstrated (*1*) for $Zr_{0.8}Yb_{0.2}F_{3.2}O_{0.3}$ ($MX_{3.5}$), using powder neutron diffraction, the structural mechanism whereby the $ReO_3$ lattice can increase the anion content above three atoms per unit cell. About one-sixth of the fluorine atoms were replaced by pairs of fluorines displaced from the ideal ($\frac{1}{2}$ 0 0) position along [100] directions. All fluorine atoms had only small displacements of about 0.3 Å toward the interior of the cell cube. The effective coordination of metal atoms sharing one such interstitial pair is increased from six to seven and they become linked by edge-shared as well as corner-shared polyhedra. The coordination of each metal atom is changed, on average, from octahedral to approximately pentagonal bipyramidal. A comprehensive discussion of possible fluorine–fluorine distances was given (*1*) to permit the distinction between favorable and unfavorable orientations of interstitial fluorines and normal fluorines. We showed that the probable limit of nonstoichiometry was between $MX_{3.7}$ and $MX_{3.8}$, in agreement with that observed in several systems. Figure 1 shows one possible arrangement of $MX_7$ polyhedra for the composition $MX_{3.5}$ with simple cubic diffraction symmetry (probable space group $Pm3m$).

0022-4596/81/120314-15$02.00/0

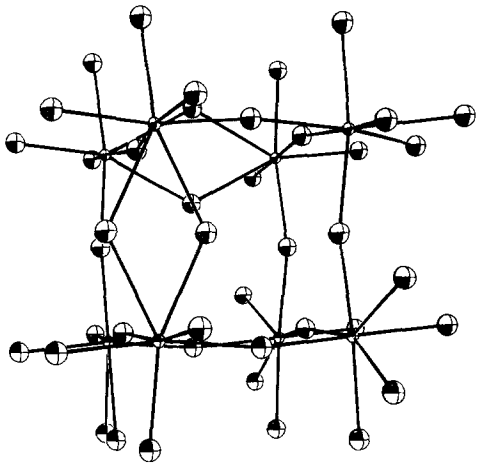

FIG. 1. A possible arrangement of $MX_7$ polyhedra, in agreement with the structural results on $Zr_{0.8}Yb_{0.2}F_{3.2}O_{0.3}$ (drawn using the ORTEP program, C. K. Johnson, ORNL Report 3794 (1965)). There is a small displacement of normal anions from the middle of the cell edges and a replacement of some of these anions by fluorine–fluorine pairs causing a change in the coordination of the neighboring metal ions from octahedral to pentagonal bipyramidal.

These results were in agreement, at least in some aspects, with the structure of $ZrO_{0.67}F_{2.67}$ ($MX_{3.33}$) (*2*). We were not aware of this work at the time of our earlier experiments. Of particular note was the absence, in both phases, of any indications of anion ordering such as was observed for some other compositions in the $ZrO_2$–$ZrF_4$ system (*2*), and as has been observed in some anion-excess fluorite systems (*3*). In the case of $ZrO_{0.67}F_{2.67}$, anion disorder, rather than order, was supported (*2*) by ir measurements.

A particular feature of the structure of $Zr_{0.8}Yb_{0.2}F_{3.2}O_{0.3}$ was that the interstitial pair separation was fairly short, 2.23(2) Å. Although such short distances have been reported in a number of structures, fluorine–fluorine distances in crystals are generally greater than 2.4 Å, although separations of between 2.3 and 2.4 Å are commonly observed for bridging fluorines separating two $ZrF_n^{(n-4)-}$ polyhedra ($n$ = 7 or 8). We have, therefore, examined other anion-excess $ReO_3$ phases, where no oxygen is present, to determine the separation between interstitial fluorines. Other questions of interest for these phases concern the generality of the defect mechanism, any evolution of the structural details with composition and degree of nonstoichiometry, and the effect of temperature on the structure and the possible transformation to more ordered structures as ionic motion becomes possible.

In this paper, we present the room-temperature structure of cubic, disordered $YbZrF_7$ where the same dopant metal is present as in the previous study. The structure has been determined both by X-rays using a single crystal, and by neutrons using a polycrystalline sample. We also show that the structure is maintained on heating to about 200°C, but that near 400°C there is a slow transformation to a more ordered structure.

## Anion-Excess $ReO_3$ Phases

The existence of anion-excess $ReO_3$-type phases has been demonstrated for $ZrF_4$ in particular, and also for $NbF_5$, in combination with alkaline-earth and transition-metal fluorides, rare-earth fluorides and oxides, and some transition-metal oxides (*2, 4–11*). Although the composition range varies from system to system, the whole range from anion-deficient $ReO_3$ structures to an anion excess of nearly 30% ($MX_{3.8}$) is encompassed, so that the domain of nonstoichiometry possibly achievable is very large. This is a result of the non-closed-packed nature of the $ReO_3$ lattice, and the presence of metal ions, particularly $Zr^{4+}$, which readily tolerate six-, seven-, and eightfold coordination by fluorine.

Structures both with and without cation ordering are found. Such ordering is favored by a large difference of charge between the host and dopant cations. In the

$MF_2$–$ZrF_4$ systems (*7*, *9*) ($M$ = Mg, Ca, Mn–Ni, Zn), for example, the nonstoichiometric domain exists for $0 \leq x \leq 0.6$ for $MX_{3+x}$ in all cases. Only for the $CaF_2$, $FeF_2$ and $CoF_2$-doped systems, however, at high fluorine compositions with Zr/Ca > 3, were phases found with primitive cubic symmetry and a simple $ReO_3$ unit cell. For all other compositions a face-centered cubic, doubled cell was observed, indicative of metal ordering. In these studies samples were quenched to room temperature from about 850°C.

Most other cases where the phase diagram has been determined, again with quenching from between 850 and 1000°C, have involved the admixture of oxides to $ZrF_4$. In these cases, the $ReO_3$-type region does not generally encompass the stoichiometric composition $MX_3$. For example, for the rare earth oxides (*6*), composition ranges extend from $MX_{3.7}$ to $MX_{3.79}$ for doping with $Pr_2O_3$, and from $MX_{3.37}$ to $MX_{3.8}$ for doping with $Yb_2O_3$. For the lighter rare earths, only metal ordered phases were observed. For doping with $Yb_2O_3$, on the other hand, a simple-cubic domain exists from $MX_{3.37}$ to $MX_{3.72}$. Only between $MX_{3.72}$ and $MX_{3.8}$ is cation ordering observed. The lack of $ReO_3$-type phases for low $x$ in $MX_{3+x}$ in these systems is probably related to the instability of several stoichiometric oxyfluorides to disproportionation to oxide and fluoride. Thus, an $ReO_3$-type phase $ZrOF_2$ could not be prepared (*2*) by normal ceramic methods, $NbOF_2$ apparently does not exist (*12*) and $SnOF_2$ disproportionates to $SnO_2$ and $SnF_4$ at 350°C (*13*). The formation of cubic phases is, without doubt, favored when the dopant ion is of a similar size to $Zr^{4+}$. There is then no strong driving force toward the formation of polyhedra of larger coordination number around the dopant ion—probably ninefold around the lighter rare earths—than around the zirconium ion.

The only situation observed hitherto with oxide doping where the range of nonstoichiometry does encompass the ideal $MX_{3.0}$ composition is for doping with $NbO_2$, where $-0.1 \leq x \leq 0.14$ for $MX_{3+x}$ (*5*). This would seem to be related in some way to the particular bonding or structural features in this system, even though an $ReO_3$-type phase $NbOF_2$ does not, apparently, itself exist (*12*). Although neither single-crystal X-ray nor electron diffraction studies revealed any indications of long-range ordering above the simple primitive cubic cell, an X-ray structure determination carried out (*14*) on a single crystal of $Nb_{0.55}Zr_{0.45}O_{1.1}F_{1.8}$ ($MX_{2.9}$) revealed that the anion disposition was more complex than expected for random vacancies on an otherwise regular sublattice. $TiO_2$, by contrast (*5*), forms a solid solution with $ZrF_4$ only between $MX_{3.33}$ and $MX_{3.74}$.

In the case of the addition of rare-earth fluorides to $ZrF_4$, only the $SmF_3$–$ZrF_4$ (*7*) and $YbF_3$–$ZrF_4$ (*9*) systems have been fully studied. The former at 900°C, and the latter at 700°C revealed no solid solution between $MF_{3.0}$ and $MF_{3.5}$. A monoclinic phase based on the $SmZrF_7$ structure (*8*) extended in both cases from $MF_{3.5}$ to $MF_{3.66}$. This structure, formed by all the rare-earth ions and yttrium, has both perfect metal and fluorine ordering (*8*) with sixfold-coordinate zirconium and eightfold-coordinate rare earth. For $YbF_3$-doping, however, quenching from 1000°C revealed a simple-cubic $ReO_3$ phase extending from about $MF_{3.4}$ to $MF_{3.7}$. It had been shown previously (*8*) that $ReO_3$-related phases could be obtained at the $MF_{3.5}$ composition ($LnZrF_7$, $Ln$ = rare earth) for the smaller rare-earth ions Er, Tm, Yb and Lu, with quenching from a lower temperature being possible as the ionic radius of the rare earth decreased. This behavior corresponds with the behavior observed for oxide additions as the ionic radius of the rare earth approaches that of $Zr^{4+}$, although for a given value of $x$ in $MX_{3+x}$, higher quenching temperatures

are necessary for fluoride doping than for oxide doping, owing to the greater degree of substitution needed by the larger rare-earth ion. Depending on the quench temperature, either an apparently face-centered cell indicating, at least partial, metal ordering, or a simple cubic $ReO_3$ phase is formed. $YbZrF_7$ is simple-cubic for quenching from 1000°C.

The structure of a nonstoichiometric fluoride-excess $ReO_3$ material with cation ordering has not yet been determined. We mention below some aspects of these materials. Many similarities are likely, however, with the metal-disordered, primitive-cubic phases discussed here.

### Sample Preparation and Data Collection

Polycrystalline $YbZrF_7$ was prepared from equimolar amounts of $YbF_3$ and $ZrF_4$ by heating in a sealed nickel tube to 1000°C for 2 days and quenching in cold water. The elementary fluorides were prepared by fluorinating the oxides at 200°C with excess ammonium bifluoride.[1] The residual $NH_4HF_2$ was removed by evacuation at higher temperature. Using pure materials it was necessary to quench from 1000°C to obtain a product showing no evidence of super-lattice ordering. A somewhat lower temperature is satisfactory if less pure materials containing transition metal impurities are used.

The room temperature lattice constant determined (Cu$K\alpha$ radiation) with an ISA X-ray diffractometer was 4.067(1) Å.

In several preparations, crystals large enough for study by X-ray diffraction could be obtained. Crystals showing both metal ordering (face-centred reflections) and no metal ordering (primitive reflections only) were examined using both photographic methods and diffractometry. A feature observed on some crystals of both types was an apparent lowering of symmetry. This was evident from intensity differences between (cubic) equivalent reflections observed in diffractometry of spherically-ground crystals. Other manifestations of symmetry-lowering, in particular, line splitting, were not generally observed, however, either in single-crystal or powder X-ray diffraction at room temperature. Such effects could well arise from preferential ordering of the interstitial defects in particular directions or intergrowth of ordered or partially ordered domains, which may be more easily achieved in larger crystallite sizes where the rate of quenching would be limited by the thermal conductivity of the crystal. As we discuss below, however, we do not believe that such ordering effects are important in the interpretation of our results on these high-temperature disordered phases and no other manifestations of ordering have been observed. The crystal used in the structure-determination study was one which showed no indications of any sort of ordering process.

A roughly cubic crystal of approximately 0.06 mm edge was selected. Intensity data were collected from a CAD 4 Nonius diffractometer using Mo$K\alpha$ radiation ($\lambda$ = 0.711 Å) and $\Omega$ scanning. The lattice parameter was 4.071 Å, but this value is less accurate than that obtained on the powder sample (4.067(1) Å). Five hundred seventy-nine intensities were collected in the angular range $5° < \theta < 50°$, giving 83 independent reflections (space-group $Pm3m$). The average relative variation of equivalent reflections was 13%. Reflections for which the standard deviation was greater than the limit $0.6I$ were not used. Structure refinement was effected using a least-squares program minimizing the function:

$$\frac{\Sigma w(F_{cal} - F_{obs})^2}{\Sigma w F_{obs}^2}.$$

[1] $ZrO_2$: CEZUS (PUK), optical grade; $Yb_2O_3$: 3 *N*, Rhone Poulenc Chimie Fine; $NH_4HF_2$: Normapur, PROLABO.

In the case of highly correlated variables, the calculated increments were divided by 5 or 8 to expedite convergence. An absorption correction was not necessary because of the low value of $\mu R$ (0.85).

Neutron diffraction was undertaken on the ILL DlA diffractometer (*15*), wavelength 1.2056(3) Å (determined from the lattice constant of $YbZrF_7$ found using X-ray powder diffraction). The sample was in a sealed vanadium can, diameter 12 mm. The data were recorded on eight counters at 6° $2\theta$ separation and precise relative counter efficiencies and separations were determined by comparing the intensities and centres of the four strongest reflections for all eight counters determined by Gaussian fitting. Peaks were observed up the (520) reflection at 105.91° $2\theta$ (room temperature). The complete $2\theta$ range to include this reflection was scanned by all eight counters at room temperature. Data were also collected subsequently at 220 ± 20°C and 390 ± 20°C (two successive scans) using a vanadium-element furnace. A more restricted scan from 45° $2\theta$ to 115° $2\theta$ for the highest angle counter was used at the higher temperature.

Intensities of all peaks were obtained by manual integration of the corrected summed data and standard deviations determined from the counting statistics. The diffraction patterns of the summed, normalized data at the various temperatures are shown in Fig. 2. It is seen that the room temperature structure is maintained at 220°C but that a slow structural transformation occurs at 390°C. The lattice constant at 220°C was 4.071(1) Å.

The structures at room temperature and 220°C were refined using the Harwell 'TAILS' program (*16*). This minimizes the agreement factor

$$\mathrm{AF} = \frac{\Sigma_j w_j (I^j_{\mathrm{obs}} - I^j_{\mathrm{calc}})}{(n - m)},$$

where $w_j$ is the weight $(1/\sigma_j^2)$ of an observed peak intensity, $I^j_{\mathrm{obs}}$, determined from counting statistics, $I^j_{\mathrm{calc}}$ is the calculated peak intensity, $n$ is the number of intensities used in the refinement and $m$ the number of parameters varied. The program also determines conventional and weighted reliability factors based on intensities. Scattering lengths of 0.714 (Zr), 1.28 (Yb), and 0.565 (F), all $\times 10^{-12}$ cm, were used.

## Results and Discussion

### *Diffraction Refinements*

The structural details are very similar to those found in the earlier work (*1*). Atom positions and isotropic temperature factors for all refinements are given in Table I. For the X-ray refinement, two models were tested: with an average metal atom, and with Zr and Yb allowed to have different locations with the same positional symmetry. The positions found are very similar in the two cases and we conclude that the two ions are not greatly differentiated in the structure.

The fluorine positional parameters are very similar for all the room temperature refinements. Although there is some variation in the fluorine occupation numbers these provide, on the whole, strong support for the model already established which would give, ideally, occupations of 2.50 for F1 and 1.00 for F2. Particularly for F2, which is less well defined than F1, there is high correlation between the thermal parameter and occupation number. In all cases, quite good refinements could have been made with fluorine occupations fixed at the ideal values, and it would be difficult to provide significant improvement by introducing extra fluorine sites as in Ref. (*2*) or to give meaningful occupations for more than two sites. We conclude that the neutron and X-ray results are in good agreement. The X-ray data provide for more accurate determination of the metal posi-

TABLE I

$YbZrF_7$ ($Pm3m$): POSITIONAL[a] AND THERMAL PARAMETERS AND OCCUPATIONS

| Atom | Position | $x$ | $y$ | $z$ | $B$ (Å$^2$) | Occupation per unit cell |
|---|---|---|---|---|---|---|
| | | | Single Crystal X Ray—Zr, Yb Independent | | | |
| Zr | 6*e* | 0.0 | 0.0 | 0.0438(15) | 2.25(41) | 0.5 |
| Yb | 6*e* | 0.0 | 0.0 | 0.0486(26) | 3.00(33) | 0.5 |
| F1 | 12*j* | 0.5 | 0.0491(13) | 0.0491 | 1.70(17) | 2.42(9) |
| F2 | 24*l* | 0.5 | 0.298(10) | 0.053(11) | 3.91(75) | 1.50(23) |
| | | | $R_f = 0.0290$ | $wR_f = 0.0322$ | | |
| | | | Single-Crystal X Ray—Average Zr/Yb | | | |
| Zr/Yb | 6*e* | 0.0 | 0.0 | 0.04366(61) | 2.17(11) | 1.0 |
| F1 | 12*j* | 0.5 | 0.0496(13) | 0.0496 | 2.55(18) | 2.30(11) |
| F2 | 24*l* | 0.5 | 0.310(15) | 0.062(16) | 4.86(1.16) | 1.07(32) |
| | | | $R_f = 0.0325$ | $wR_f = 0.0341$ | | |
| | | | Neutron Data—Room Temperature | | | |
| Zr/Yb | 6*e* | 0.0 | 0.0 | 0.060(14) | 1.71(96) | 1.0 |
| F1 | 12*j* | 0.5 | 0.052(3) | 0.052 | 3.10(44) | 2.66(12) |
| F2 | 24*l* | 0.5 | 0.289(9) | 0.064(8) | 3.02(1.66) | 0.78(15) |
| | | | $R_I = 0.0322$ | $wR_I = 0.0483$ | | |
| | | | Neutron Data—220°C | | | |
| Zr/Yb | 6*e* | 0.0 | 0.0 | 0.071(12) | 1.73(1.07) | 1.0 |
| F1 | 12*j* | 0.5 | 0.047(5) | 0.047 | 3.22(50) | 2.36(13) |
| F2 | 24*l* | 0.5 | 0.261(12) | 0.094(6) | 6.12(1.90) | 1.31(25) |
| | | | $R_I = 0.0330$ | $wR_I = 0.0518$ | | |

[a] Atomic positions are in fractions of the unit cell edge ($a$ = 4.072 Å, single crystal, and 4.067 Å, powder, room temperature; 4.071 Å powder, 220°C).

tions but the errors on the fluorine positions are comparable in the two cases. The greater sensitivity of neutrons to the light element roughly compensates the smaller data set collected in a powder diffraction experiment.

*Fluorine–Fluorine Separations*

As in $Zr_{0.8}Yb_{0.2}F_{3.2}O_{0.3}$, the fluorine ions are not significantly displaced toward the interior of the cell. For $YbZrF_7$ at room temperature, however, the F2–F2 separations are not at all unusually short. For the best X-ray and neutron refinements, the longest separations are 2.46(10) Å and 2.41(8) Å, respectively. These values agree closely within one standard deviation and are comparable to F–F distances for pairs shared by $ZrF_n^{(4-n)-}$ polyhedra (Table II). Thus the primitive cubic, disordered $MF_{3+x}$ structure can indeed show "normal" F–F distances for all atoms. The value for the F2–F2 separation found (1) for $Zr_{0.8}Yb_{0.2}F_{3.2}O_{0.3}$ (2.23(2) Å) cannot, therefore, be an artifact of the diffraction technique used. It remains for further work to establish the range of values which can be found and whether the presence of oxygen might play some role in modifying the apparent distance. Perhaps more likely, the enlargement of the unit cell for $YbZrF_7$, compared to $Zr_{0.8}Yb_{0.2}F_{3.2}O_{0.3}$, arising from the higher level of doping with $Yb^{3+}$, is the main factor permitting an expansion of the F2–F2 pair. We should note that distances close to 2.2 Å for F–F separations have been reported both for a $ZrF_8^{4-}$ polyhedron in $PbZrF_6$ (Table II) and in borofluorides

TABLE II

SOME Zr–F AND F–F BOND DISTANCES IN ZIRCONIUM FLUORIDES

| Compound | Average Zr–F distance (Å) | F–F separation for shared pair (Å) | Method of linking $ZrF_n^{(4-n)-}$ polyhedra | Ref. |
|---|---|---|---|---|
| | | Octahedral $ZrF_6^{2-}$ | | |
| $SmZrF_7$ | 2.006 | | Isolated octahedra | [a] |
| $Li_2ZrF_6$ | 2.016 | | Isolated octahedra | [b] |
| $CuZrF_6 \cdot 4H_2O$ | 1.995 | | Isolated octahedra | [c] |
| $Rb_5Zr_4F_{21}$ | 1.985 | | Isolated octahedra | [d] |
| | | Sevenfold Coordinate $ZrF_7^{3-}$ | | |
| $(NH_4)_3ZrF_7$ | 2.02* | | Isolated $ZrF_7^{3-}$ | [e] |
| $Na_5Zr_2F_{13}$ | 2.06 | | Corner-linked $Zr_2F_{13}^{5-}$ dimers | [f] |
| $\gamma$-$Na_2ZrF_6$ | 2.065 | | Corner-linked chains of $ZrF_7^{3-}$ groups | [g] |
| $K_2Cu(ZrF_6)_2 \cdot 6H_2O$ | 2.063 | 2.327(6) | Edge-shared $Zr_2F_{12}^{4-}$ dimers | [h] |
| $BaZrF_6$ | 2.082 | 2.36 | Edge-shared $Zr_2F_{12}^{4-}$ dimers | [i] |
| $Rb_5Zr_4F_{21}$ | 2.063 | 2.34(2) | One edge-shared with $ZrF_6^{4-}$ unit | [d] |
| $Rb_5Zr_4F_{21}$ | 2.076 | 2.32(2) | One edge-shared with $ZrF_8^{4-}$ unit | [d] |
| | | Eightfold Coordinate $ZrF_8^{4-}$ | | |
| $Li_6BeZrF_{12}$ | 2.015 | | Isolated $ZrF_8^{4-}$ | [j] |
| $Cu_2ZrF_8 \cdot 12H_2O$ | 2.103 | | Isolated $ZrF_8^{4-}$ | [k] |
| $Cu_3(ZrF_7)_2 \cdot 16H_2O$ | 2.086 | 2.35 | Edge-shared $Zr_2F_{14}^{6-}$ dimers | [l] |
| $ZrF_4 \cdot 3H_2O$ | | 2.367(4) | F–F bridge between $Zr_2F_8(H_2O)_6$ dimers | [m] |
| $Rb_5Zr_4F_{21}$ | 2.114 | 2.34(2) and 2.32(2) | Two edges shared with $ZrF_7^{3-}$ units | [d] |
| $Na_7Zr_6F_{31}$ | 2.113 | 2.38 | $ZrF_8^{4-}$ units share corners and one edge | [n] |
| $K_2ZrF_6$ | 2.114 | 2.372 | Chains of $ZrF_8^{4-}$ units | [o] |
| $PbZrF_6$ | 2.095 | 2.23 | Chains of $ZrF_8^{4-}$ units | [p] |
| $N_2H_6ZrF_6$ | 2.118 | 2.40(5) and 2.46(4) | Chains of $ZrF_8^{4-}$ units | [q] |

* This structure is disordered: the possible average Zr–F distance given would appear to be too short by comparison with other $ZrF_7^{3-}$ systems.

[a] See Ref. (*8*).

[b] G. BRUNTON, *Acta Crystallogr. Sect. B* **29**, 2294 (1973).

[c] J. FISCHER AND R. WEISS, *Acta Crystallogr. Sect. B* **29**, 1955 (1973).

[d] G. BRUNTON, *Acta Crystallogr. Sect. B* **27**, 1944 (1971).

[e] H. J. HURST AND J. C. TAYLOR, *Acta Crystallogr. Sect. B* **26**, 417 (1970).

[f] R. M. HERAK, S. S. MALCIC, AND L. M. MANOJLOVIC, *Acta Crystallogr.* **18**, 520 (1965).

[g] G. BRUNTON, *Acta Crystallogr. Sect. B* **25**, 2164 (1969).

[h] J. FISCHER AND R. WEISS, *Acta Crystallogr. Sect. B* **29**, 1958 (1973).

[i] J. P. LAVAL, R. PAPRERNIK, AND B. FRIT, *Acta Crystallogr. Sect. B* **34**, 1070 (1978).

[j] D. R. SEARS AND J. H. BURNS, *J. Chem. Phys.* **41**, 3478 (1964).

[k] J. FISCHER, R. ELCHINGER, AND R. WEISS, *Acta Crystallogr. Sect. B* **29**, 1967 (1973).

[l] J. FISCHER AND R. WEISS, *Acta Crystallogr. Sect. B* **29**, 1963 (1973).

[m] F. GABELA, B. KOJIC-PRODIC, M. SLJUKIC, AND Z. RUZIC-TOROS, *Acta Crystallogr. Sect. B* **33**, 3733 (1977).

[n] J. H. BURNS, R. D. ELLISON, AND H. A. LEVY, *Acta Crystallogr. Sect. B* **24**, 230 (1968).

[o] R. HOPPE AND B. MEHLHORN, *Z. Anorg. Chem.* **425**, 200 (1976).

[p] J. P. LAVAL, D. MERCURIO-LAVAUD, AND B. GAUDREAU, *Rev. Chim. Miner.* **11**, 742 (1974).

[q] B. KOJIC-PRODIC, S. SCAVINKAR, AND B. MATKOVIC, *Acta Crystallogr. Sect. B* **27**, 638 (1971).

such as $NH_4BF_4$ (2.279(8) Å, Ref. (*17*)) and $N_2H_5BF_4$ (2.166(20) Å to 2.225(21) Å, Ref. (*18*)).

Inspection of the possible fluorine–fluorine separations between the two types of fluorine ions on neighboring sites yields the same conclusions as in Ref. (*1*), where a comprehensive discussion was given. There are no constraints for neighboring F1 atoms while for the closest F1 set (for example around (0 ½ 0)—see Ref. (*1*), Fig. 4) to an F2 atom at (½ *y z*) the two longer separations will be favored. This is the only constraint on F2–F1 separations. For neighboring F2 atoms the constraints are more severe but no neighboring sites are totally excluded. For an F2 at (½ *y z*), for example, there seems only one possible orientation for a pair centred at (0 ½ 0) or (1 ½ 0) (see Fig. 5, Ref. (*1*)), two forbidden orientations for a pair centred at (½ 1 0) and one forbidden orientation for a pair centred at (0 0 ½) or (1 0 ½). All F–F separations less than 3 Å, for fluorines on neighboring sites, are given in Table III for the best X-ray refinement with separate Zr and Yb positions and for the neutron refinement at room temperature. The values all agree to within 0.1 Å and generally to less than 0.05 Å. Although the calculated standard deviations are generally less than this, a confidence of 0.05–0.1 Å is probably reasonable. The structural interpretations from the two data sets are the same. The only small change compared to $Zr_{0.8}Yb_{0.2}F_{3.2}O_{0.3}$, resulting from the longer F2–F2 separation in $YbZrF_7$, is that the closest neighboring F2–F1 distances are now essentially the same as the F2–F2 pair separation.

*Metal–Fluorine Distances*

We showed previously (*1*) that the average metal–fluorine distance in $Zr_{0.8}Yb_{0.2}F_{3.2}O_{0.3}$ was very close to that expected. Assuming a coordination number of seven with five F1 and two F2 neighbors, and F1 positions determined by favorable F2–F1 separations, it is likely that there is more than one possible *M*–F distance for only two of the five F1 neighbors (Figure 6 of Ref. (*1*)). There is, therefore, very little uncertainty in the average *M*–F distance in this structure. Assuming that in the present refinements with an average metal atom the longer separation would correspond to a Yb–F polyhedron and the shorter to a Zr–F polyhedron, the average Yb–F and Zr–F separations (in Å) calculated in the three room temperature refinements are:

| | Yb–F = | Zr–F = |
|---|---|---|
| X rays, separate Zr, Yb | 2.145 | 2.134 |
| X rays, average Zr/Yb | 2.154 | 2.144 |
| Neutrons, average Zr/Yb | 2.142 | 2.127 |

These are all closely similar. Relatively small shifts of the metal positions which could maintain reasonable individual *M*–F bond lengths do not, in fact, change the average separation to any significant degree. This is presumably why the positions of Yb and Zr, when refined separately, lie only just outside one standard deviation apart, and explains the absence of diffuse scattering under the (100) reflection (Fig. 2) which would be expected if the metal–metal separations varied significantly from cell to cell. This is in contrast to the situation observed (*19*) in $ZrF_4$-based glasses.

We notice that the average Zr–F separations are all longer than found in more ordered materials (Table II) even for eightfold coordinated zirconium. Conversely, the average Yb–F separations are all shorter than expected; the ionic radius of $Yb^{3+}$ is about 0.15 Å greater than that of

TABLE III

CLOSEST FLUORINE–FLUORINE SEPARATIONS IN $YbZrF_7$ AT ROOM TEMPERATURE

| First fluorine[a] | Second fluorine[a] | Best X-ray refinement (Zr, Yb independent) (Å) | Neutron refinement (Average Zr/Nb) (Å) |
|---|---|---|---|
| F1 (0.5 $x$ $x$) | F1 ($x$ ½ $x$) (1)[b] | 2.596 | 2.577 |
| | ($x$ ½ $-x$) (2) | 2.627 | 2.611 |
| | ($-x$ ½ $x$) (3) | 2.893 | 2.891 |
| | ($-x$ ½ $-x$) (4) | 2.920 | 2.922 |
| F2 (0.5 $y$ $z$) | F1 ($x$ ½ $x$) (1) | 2.013 | 2.015 |
| | ($x$ ½ $-x$) (2) | 2.055 | 2.069 |
| | ($-x$ ½ $x$) (3) | 2.383 | 2.404 |
| | ($-x$ ½ $-x$) (4) | 2.414 | 2.449 |
| | F1 (½ 1 − $x$ $x$) | 2.660 | 2.681 |
| | (½ 1 − $x$ $-x$) | 2.692 | 2.721 |
| | F1($x$ $x$ ½)(A) | 2.777 | 2.719 |
| | ($x$ $-x$ ½) (B) | 2.946 | 2.896 |
| F2 (0.5 $y$ $z$) | F2 ($y$ ½ $z$) (1) | 1.166 | 1.214 |
| | ($y$ ½ $-z$) (2) | 1.242 | 1.321 |
| | ($z$ ½ $y$) (3) | 2.212 | 2.172 |
| | ($z$ ½ $-y$) (4) | 2.456 | 2.438 |
| | ($-z$ ½ $y$) (5) | 2.596 | 2.614 |
| | ($-z$ ½ $-y$) (6) | 2.788 | 2.839 |
| | F2 ($y$ $z$ ½) (1) | 2.234 | 2.172 |
| | ($y$ $-z$ ½) (2) | 2.456 | 2.438 |
| | ($z$ $y$ ½) (3) | 2.576 | 2.508 |
| | ($-z$ $y$ ½) (4) | 2.895 | 2.899 |
| | F2 (½ 1 − $y$ $z$) (1) | 1.649 | 1.716 |
| | (½ 1 − $y$ $-z$) (2) | 1.704 | 1.793 |
| | (½ 1 − $z$ $y$) (3) | 2.828 | 2.786 |
| | F2 (½ $z$ 1 − $y$) | 2.828 | 2.786 |

[a] Positions correspond to those given in Table I.

[b] Numbers or letters in parentheses show correspondence with Figs. 4 and 5 and Tables III and IV of Ref. (*1*).

$Zr^{4+}$. This mismatch, inevitable on a statistical basis in a primitive cubic compound of this type is probably a dominant reason controlling the stoichiometry ranges accessible by conventional synthetic methods and determines that the compositions are stable only at elevated temperatures. We have mentioned above that these phases become relatively more stable as the ionic radius of the dopant ion approaches that of $Zr^{4+}$.

It might be expected that there would be maximum stability for dopant ions such as $Sc^{3+}$ (0.885 Å), $Ti^{3+}$ (0.810 Å), $Mo^{3+}$ (0.83 Å) or $Nb^{5+}$ (0.78 Å) whose ionic radii (Ref. (*20*), values are given for sixfold coordination) are closer to that of $Zr^{4+}$ (0.86 Å) than are those of the rare earths ($Yb^{3+}$: 1.008 Å; $Lu^{3+}$: 1.001 Å). Preliminary experiments (*21*) have indeed shown wide solubility ranges for doping of $ZrF_4$ with $ScF_3$, $TiF_3$ and $NbO_2F$ although the unit cells were not primitive-cubic and contained more than one formula unit.

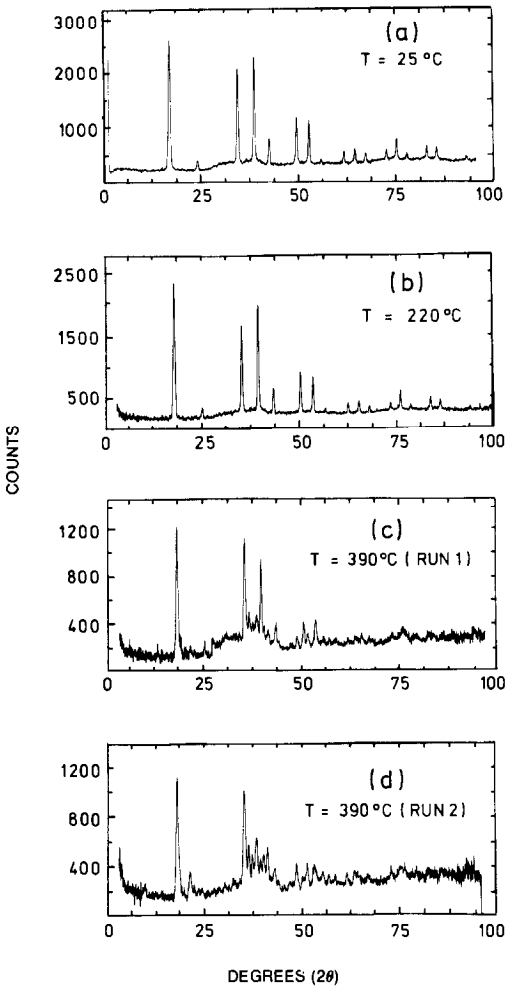


FIG. 2. Diffraction patterns of polycrystalline $YbZrF_7$, D1A diffractometer, ILL Grenoble. (a), (b) at room temperature and 220°C respectively showing primitive cubic (one molecule per cell) reflections only; (c), (d) successive runs at 390°C showing the slow transformation to the ordered monoclinic $YbZrF_7$ structure. The data for all counters have been summed after correction for separation and relative efficiencies. For run (a), all eight counters were used; for the higher temperature runs one (b) or more counters were omitted. Small background spikes between 25 and 30° $2\theta$ (c) and between 6 and 12° $2\theta$ (d) are not significant.

### *The Fluorine Disorder and Comparison with Related Phases*

The local organization of the fluorine substructure will certainly be influenced by the need to adjust metal–fluorine distances as well as by the fluorine–fluorine interactions themselves. A prominent feature of all the compositions of this type we have studied by neutron diffraction, which is particularly sensitive to the light atoms, is a region of diffuse scattering commencing to the high angle of the (110) reflection and tailing off by the (211) reflection (Fig. 2; Fig. 2 of Ref. (*1*)). In fact, in $YbZrF_7$, at room temperature (Fig. 2a), this diffuse scattering is rather clearly resolved into two components centered around 32.5° $2\theta$, and near 39° $2\theta$ under the (210) reflection. If we follow the formula discussed by Guinier (*22*):

$$1.23\lambda = 2d \sin \theta,$$

then these diffuse peaks correspond to average separations near 2.65 and 2.20 Å, respectively. These fall within the ranges of values for near-neighbor fluorine–fluorine and metal–fluorine contacts respectively and it seems very reasonable to assign their origin to variations in such distances from cell to cell in the light of the discussion already given. By contrast, for the oxyfluoride studied previously, only the fluorine–fluorine peak was particularly prominent. This difference probably arises from the higher dopant level of $Yb^{3+}$ in the present case, 50% compared to 20%.

We have mentioned the almost perfect positional order observed on the metal sublattice. The partial disorder on the fluorine sublattice, evident by the presence of the diffuse scattering shows that the anion-excess, primitive-cubic compositions of the type we have studied may be viewed as phases with an order intermediate between compounds such as $SmZrF_7$ (*8*), where there is perfect order on both sublattices, and the fluoride glasses based on $ZrF_4$ (*23*), where the presence of modifier cations of large ionic radius permits the destruction of long-range order on the cation sublattice as well as on the anion sublattice. Common both to the glasses and to the crystalline disor-

dered phases is the presence of a large numerical excess of monovalent fluorine anions over highly charged cations, and the ability of zirconium, as seen from the examples in Table II, readily to adapt its coordination by fluorine between six and eight. Although covalent interactions between $Zr^{4+}$ and $F^-$, mentioned in Ref. (*1*) may play a role, they are probably not dominant as in the case of silicate and related glasses. In the zirconium fluorides the large Coulombic attractions between nearest-neighbor anions and cations are maximized by the large coordination numbers, greater than six, in the disordered phases but the lattice energy is lowered by the large number of negative fluorine–fluorine interactions which reduces the tendency to form well-ordered, crystalline phases. Thus, for the fluorides of such ions as $Zr^{4+}$ and $Nb^{5+}$, we observe low sublimation temperatures or the ready formation of liquid phases (e.g., $NbF_5$: melting point 80°C), as well as the preparation of glasses and partially disordered crystalline solids.

For $Zr^{4+}$, Coulombic repulsion between neighboring $Zr^{4+}$ ions does not prevent the formation of shared fluorine pairs, and these seem to be essential to the existence of phases of the type discussed here. Many examples found in well-ordered crystalline compositions are also given in Table II. In contrast, the smaller, more-highly charged $Nb^{5+}$ cation does not show such behavior. Although fewer niobium fluorides have been studied than is the case for zirconium, we are not aware of any situations where niobium–fluorine polyhedra are linked by more than one bridging fluorine. Some examples are given in Table IV. The average Nb–F separations for six- and sevenfold coordination by fluorine are about 0.1 Å shorter than is the case with Zr–F. Already, as is shown with $K_2NbF_7$, this produces a rather short F–F separation of 2.357(4) Å for an isolated $NbF_7^{2-}$ unit. The increased metal–metal repulsion arising from the higher metal-ion charge on the one hand, and the very short F–F separation expected for a shared pair arising from the smaller metal–fluorine separations on the other hand, explain why such pairs do not seem to be observed.

This difference is of interest with regard

TABLE IV

SOME Nb–F AND F–F BOND DISTANCES IN NIOBIUM FLUORIDES

| Compound | Average Nb–F distance (Å) | Closest F–F separation (Å) | Method of linking $NbF_7^{(5-n)-}$ polyhedra | Ref. |
|---|---|---|---|---|
| $SeF_4 \cdot NbF_5$ | 1.84<br>1.90 | 2.46(4) | $NbF_6^-$ linked to $SeF_3^+$ units to form $Nb_4F_{20}$-like tetramers | [a] |
| $SbF_5 \cdot NbF_5$ | 1.93 | 2.49(2) | Chains of corner-linked $SbF_6^-$ and $NbF_6^-$ | [b] |
| $SeF_4 \cdot 2NbF_5$ | 1.87<br>1.88 | >2.5 | Corner-linked $Nb_2F_{11}^-$ dimers | [c] |
| $NbF_5$ | 1.86<br>1.87 | >2.5 | Corner-linked $Nb_4F_{20}$ tetramers | [d] |
| $K_2NbF_7$ | 1.959 | 2.357(4) | Isolated $NbF_7^{2-}$ | [e] |

[a] A. J. EDWARDS AND G. R. JONES, *J. Chem. Soc. A*, 1891 (1970).
[b] A. J. EDWARDS, *J. Chem. Soc. (Dalton)*, 2325 (1972).
[c] A. J. EDWARDS AND G. R. JONES, *J. Chem. Soc. A*, 1491 (1970).
[d] A. J. EDWARDS, *J. Chem. Soc.*, 3714 (1964).
[e] G. M. BROWN AND L. A. WALKER, *Acta Crystallogr.* **20**, 220 (1966).

to anion-excess $ReO_3$ phases based on $NbF_5$, which always show metal ordering. It must be assumed that similar structural principles are involved, particularly the presence of shared F–F pairs, as in the case of the primitive-cubic, metal-disordered phases. Several examples of metal-ordered phases involving $NbF_5$ are known, for example $MNbF_7$ where $M$ = Mg, Ca, Mn, Fe, Co, Ni, Zn (*10, 11*). The doubling of the unit cell, although permitting ordering of the metal ions, does not permit an ordering of the fluorine sublattice. In the case of $ZrF_4$, wide regions of stability, often $ZrF_4$-rich, are observed with fcc symmetry (see above), and shared F–F pairs between neighboring $Zr^{4+}$ ions probably occur. For fcc $YbZrF_7$ moreover, an X-ray study of a single crystal showed (*24*) clearly that the metal-ordering was by no means perfect, although, as discussed above, inequivalences in nominally equivalent reflections did not permit a full resolution of the structure. The determination and interpretation of a disordered structure eight times the volume of the primitive cells discussed here would anyway be difficult. For the $NbF_5$-based compounds, however, a more perfect metal ordering is likely, both because of the greater charge difference between cations, and because of the need to prevent shared pairs occurring between neighboring niobium atoms. This further restriction for $Nb^{5+}$ probably helps to explain why, in the case of $MnF_2$–$NbF_5$, for which the phase diagram was studied (*10*), the fcc $MnNbF_7$ compound is only a line phase, and also implies that primitive-cubic fluorine-excess phases based on $NbF_5$ will not readily be prepared.

*Results at 220 and 390°C*

The diffraction pattern at 220°C (Fig. 2) shows clearly that the room temperature structure is maintained. The counting statistics are not as good at the higher temperature, because of a more rapid scan, but the refinement results are in overall agreement with the low temperature set (Table I). The only, possibly significant, changes are in the position, temperature factor and occupation of F2. The latter is increased at the expense of F1. There is, however, a very high correlation, about 90%, between B and the occupation of F2. In the light of the changes observed at 390°C, it is possible that these results could be interpreted as the production of an increased number of F2–F2 pairs with, presumably, some fluorine vacancies, which could lead to the possibility of metal diffusion and the onset of long-range ordering of Zr and Yb. The individual fluorine occupations are still close to the ideal values within just over one standard deviation, however, so that such a conclusion must remain conjectural at present. These results do indicate that an accurate diffraction study as a function of temperature would be interesting. The F2–F2 pair separation is reduced somewhat to 2.26(11) Å, but again, this overlaps the room temperature value from neutron diffraction (2.41(8) Å) within one standard deviation, so no significance can be placed on the change.

In contrast, a slow structural change is proceeding at 390°C. The composition was invariant as a gold 'O' ring seal on the sample can prevented any escape of $ZrF_4$. Each scan was collected in about 12 hr. In both there is a disappearance of the higher angle reflections indicating increased disorder, and only the (100) and (200) primitive-cubic reflections seem to be maintained through both scans with relatively similar intensities. Both are broadened, however, compared to the lower-temperature scans, indicating either a significant decrease in effective particle size or a small splitting into more than one line, associated with symmetry lowering. A detailed examination of the form of the (100) reflection reveals that there is a predominant non-Gaussian tail at high angle in the high-

temperature runs in contrast to the effect expected at low $2\theta$ resulting from the finite counter-aperture height, and which is seen for the (100) reflection at room temperature and 220°C. This strongly supports symmetry lowering as a cause of the broadening although effects due to reduced effective particle size may well also be present.

Particularly noticeable is the increase in the diffuse scattering intensity between 25° $2\theta$ and 45° $2\theta$ in run 1 compared to the lower-temperature data sets, indicating a considerably increased disorder on the fluorine sublattice. In the second run, however, this is becoming converted into several new reflections and a prominent new reflection at lower angle near 21° $2\theta$ has appeared.

The new lines evident on run 2 can all be indexed by reference to the X-ray diffraction pattern of monoclinic $YbZrF_7$ at room temperature, and a splitting of the (100) cubic line into three closely-spaced lines in the monclinic phase is expected. We have made no attempt to assess the expected intensities but the rate of transformation as well as the line positions support the interpretation that monoclinic $YbZrF_7$ is being formed. Although the fluorine-ion mobility in the fluorine-excess primitive-cubic phases is not particularly high, and in a few phases studied (*25*) is comparable to that reported (*26*) for fluoride glasses based on $ZrF_4$, an anion-ordering process not associated with cation ordering would involve motions of, say, 100 Å at the maximum. This would imply a diffusion constant for fluorine of $10^{-16}$–$10^{-17}$ cm$^2$/sec for the reaction time of $10^4$–$10^5$ sec actually observed. These values are many orders lower than those observed in related compounds (results extrapolate to $10^{-8}$–$10^{-9}$ cm$^2$/sec near 400°C for $ZrF_4$-based glasses (*26*)). They may not be at all unreasonable, however, for the metal-ion diffusion process which is involved in the transformation to monoclinic $YbZrF_7$.

## Conclusions

Apart from the possible evidence mentioned above, associated with the inequivalences observed in X-ray diffractometry of some cubic crystals, we have no evidence indicating the presence of any long-range anion ordering in the materials studied. Possible structures may be imagined which would permit such ordering and maintain at favorable distances all fluorine–fluorine separations. One such, for the $MX_{3.5}$ composition, is shown in Fig. 3, where all cations have seven-fold coordination. We are not aware of any related examples of such linked pentagonal bipyramids for other materials of overall composition $MX_{3.5}$. However, all such structures would lower the symmetry from cubic and enlarge

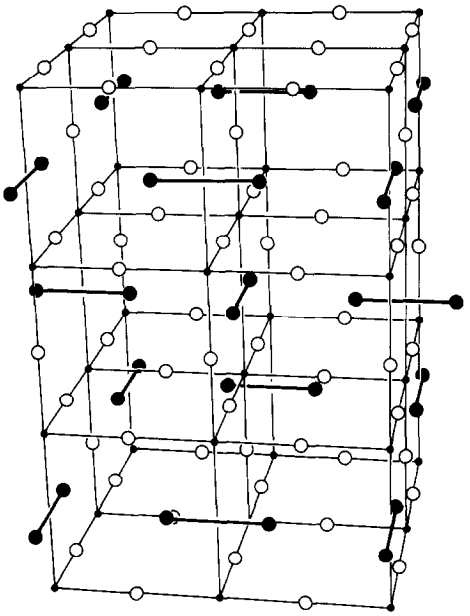

FIG. 3. One possible scheme for an $MX_{3.5}$ phase showing ordering of F2–F2 pairs (drawn using the ORTEP program, C. K. Johnson, ORNL Report 3794 (1965)). All constraints on F2–F1 and F2–F2 separations, as discussed in the text, are observed. For ease of interpretation, F1 has been placed at the (primitive cubic) ($\frac{1}{2}$ 0 0) position, and F2 at ($\frac{1}{2}$ 0.3 0). [•, metal ions (at (000)); ○, F1; and ●, F2].

the unit cell so that, as was the case with anion-excess fluorites (*3*) and the ordered phases in the $ZrO_2$–$ZrF_4$ system (*2*), some indication of ordering would be expected in the diffraction patterns. None is seen until the slow transformation to monoclinic $YbZrF_7$ commences. Although in some circumstances, for example $Sr_4Fe_4O_{11}$ (*27*), anion ordering effects are not at all readily visible in X-ray diffraction, they are immediately apparent in electron diffraction. Electron diffraction studies (*14*) of the anion-excess $ReO_3$ phases have shown no such effects and, in any case, there is little similarity between the preparation by quenching from high temperature necessary for the phases discussed here, and the careful annealing needed (*27*) to produce ordered $Sr_4Fe_4O_{11}$. Possibly, as indicated by the effects observed with some crystals, such ordering effects might be obtained by careful annealing just above or perhaps below room temperature. The overall structural features determined in this work and before (*1*) would still apply.

In conclusion, we view these crystalline anion-excess phases as characterized by a substitution of "normal" F1 atoms by F2–F2 pairs which increases the average coordination number from six to seven in the case of $YbZrF_7$ ($MX_{3.5}$). The absence of any manifestation of long-range ordering, and the diffuse scattering always observed indicate that there is no long-range ordering of the fluorine units and we consider these phases as being intermediate between well-crystallized, fully ordered phases such as monoclinic $YbZrF_7$, and the $ZrF_4$-based fluoride glasses, or liquids such as $NbF_5$, where the cation, as well as the anion sublattice, is disordered. In particular, it does not seem profitable to discuss the structure in terms of intergrown domains of ordered phases which would imply discontinuities in the solid which are both unobserved and uncharacteristic of the preparative conditions. Nor do the endmembers of any nonstoichiometric series, $MX_3$ or $MX_4$, generally fall within the range of stoichiometry observed. The structure exhibited on quenching to room temperature is maintained at around 200°C, but near 400°C, when escape of $ZrF_4$ is prevented, a slow transformation to monoclinic $YbZrF_7$ is observed.

## Acknowledgments

The encouragement of J. Lucas during the course of this work is gratefully acknowledged. We are indebted to A. W. Hewat and I. Bailey for assistance with the use of the D1A diffractometer.

## References

1. B. C. Tofield, M. Poulain, and J. Lucas, *J. Solid State Chem.* **27**, 163 (1979).
2. P. Joubert and B. Gaudreau, *Rev. Chim. Miner.* **12**, 289 (1975).
3. A. W. Mann and D. J. M. Bevan, *J. Solid State Chem.* **5**, 410 (1972).
4. H. L'Helgoualch, M. Poulain, J. P. Rannou, and J. Lucas, *C.R. Acad. Sci. Paris Ser. C* **272**, 1321 (1971).
5. J. P. Rannou, H. L'Helgoualch, and J. Lucas, *C.R. Acad. Sci. Paris Ser. C* **274**, 612 (1972).
6. F. Champlon and J. Lucas, *C.R. Acad. Sci. Paris Ser. C* **276**, 1097 (1973).
7. M. Poulain, M. Poulain, and J. Lucas, *Mater. Res. Bull.* **7**, 319 (1972).
8. M. Poulain, M. Poulain, and J. Lucas, *J. Solid State Chem.* **8**, 132 (1973).
9. M. Poulain, M. Poulain, and J. Lucas, *Rev. Chim. Miner.* **12**, 9 (1975).
10. D. Bizot and J. Chassaing, *Rev. Chim. Miner.* **13**, 139 (1976).
11. C. Monteil and J. Chassaing, *Rev. Chim. Miner.* **16**, 104 (1979).
12. H. Schäfer *et al.*, *Naturwissenshaften* **51**, 241 (1964).
13. K. Dehnecke, *Chem. Berich.* **98**, 280 (1965).
14. M. Poulain, J. Lucas, and R. J. D. Tilley, *J. Solid State Chem.* **17**, 311 (1976).
15. A. W. Hewat and I. Bailey, *Nucl. Instrum. Meth.* **137**, 463 (1976).
16. K. D. Rouse and M. J. Cooper, Harwell Report MPD/NBS/143 (1980).
17. A. P. Caron and J. L. Ragle, *Acta Crystallogr. Sect. B* **27**, 1102 (1971).

*18.* J. W. CONANT AND R. B. ROOF JR., *Acta Crystallogr. Sect. B* **26,** 1928 (1970).
*19.* M. CHANTHANASINH, Thèse de 3ème cycle, Rennes (1976).
*20.* R. D. SHANNON, *Acta Crystallogr. Sect. B* **32,** 751 (1976).
*21.* G. DENÈS, Thèse de 3ème cycle, Rennes (1973).
*22.* A. GUINIER, "Thèorie et Technique de la Radiocristallographie," 3rd ed. Dunod, Paris (1964).
*23.* M. POULAIN AND J. LUCAS, *Verres Réfract.* **32,** 505 (1978).
*24.* M. POULAIN, unpublished results.
*25.* D. ANSEL AND J. DEBUIGNE (private communication).
*26.* D. LEROY, J. LUCAS, M. POULAIN, AND D. RAVAINE, *Mater. Res. Bull.* **13,** 1125 (1978).
*27.* B. C. TOFIELD, C. GREAVES, AND B. E. F. FENDER, *Mater. Res. Bull.* **10,** 737 (1975).